



ORIGINAL ARTICLE

**During photosynthetic induction, biochemical and stomatal limitations differ between
Brassica crops**

Taylor, Samuel H.^{1*}, Orr, Douglas J.¹, Carmo-Silva, Elizabete¹, and Long, Stephen P.^{1,2}

¹Lancaster Environment Centre, Lancaster University, Lancaster, LA1 4YQ, UK

²Departments of Plant Biology and of Crop Sciences, Carl R. Woese Institute of Genomic
Biology, University of Illinois, 1206 W. Gregory Dr., Urbana, IL 61801, USA

Running title: Photosynthetic induction in *Brassica* crops

*corresponding author: s.taylor19@lancaster.ac.uk

Accepted Article

This article has been accepted for publication and undergone full peer review but has not been through the copyediting, typesetting, pagination and proofreading process which may lead to differences between this version and the Version of Record. Please cite this article as doi: 10.1002/pce.13862

Abstract

Interventions to increase crop radiation use efficiency rely on understanding how biochemical and stomatal limitations affect photosynthesis. When leaves transition from shade to high light, slow increases in maximum Rubisco carboxylation rate and stomatal conductance limit net CO₂ assimilation for several minutes. However, as stomata open, intercellular [CO₂] increases, so electron transport rate could also become limiting. Photosynthetic limitations were evaluated in three important *Brassica* crops: *B. rapa*, *B. oleracea* and *B. napus*. Measurements of induction after a period of shade showed that net CO₂ assimilation by *B. rapa* and *B. napus* saturated by 10 min. A new method of analyzing limitations to induction by varying intercellular [CO₂] showed this was due to co-limitation by Rubisco and electron transport. By contrast, in *B. oleracea*, persistent Rubisco limitation meant that CO₂ assimilation was still recovering 15 min after induction. Correspondingly, *B. oleracea* had the lowest Rubisco total activity. The methodology developed, and its application here, shows a means to identify the basis of variation in photosynthetic efficiency in fluctuating light, which could be exploited in breeding and bioengineering to improve crop productivity.

Key words

Brassica oleracea, *Brassica napus*, *Brassica rapa*, dynamic photosynthesis, Rubisco, photosynthetic electron transport, photosynthetic induction, stomata, crop improvement, CO₂ response

Introduction

The continued growth of the global human population and its increasing urbanisation will lead to increased pressure on farming systems over the next half century, and increased productivity on the land we are already using will be crucial to minimize the environmental impacts (Tilman, Balzer, Hill & Befort 2011). In this context, it is essential to understand photosynthetic efficiency because it fundamentally affects the productivity and efficiency of resource use by crops. The majority of crops use C_3 photosynthesis, which requires massive investment of nitrogen in leaf chloroplasts, where 21-74% of leaf soluble protein is allocated to the primary CO_2 fixing enzyme ribulose-1,5-bisphosphate (RuBP) carboxylase/oxygenase (Rubisco; Carmo-Silva, Scales, Madgwick & Parry 2015). Furthermore, A cost of allowing CO_2 into the leaf for photosynthesis, is the escape of water vapour via transpiration (Farquhar & Sharkey 1982; Raschke 1975). Consequently, crop biological N_2 fixation and crop applied N fertilisers now account for more than 44% of the total annual N entering the global biosphere (Fowler *et al.* 2013), and crop irrigation accounts for 70% of annual global human water use (Haddeland *et al.* 2014).

The major focus of studies of crop photosynthetic efficiency has been under light-saturating steady-state conditions. Yet these are rare for crop leaves in the field or glasshouse. Importantly, crop photosynthetic efficiency may be substantially affected by dynamic regulation in non-steady-state conditions. Adjustments to cope with changes in availability of light, e.g., caused by temporary shading within crop canopies, result in deviation from performance optima that are measured and defined in terms of steady-state conditions (Kaiser *et al.* 2016; Kromdijk *et al.* 2016; Lawson & Vialet-Chabrand, 2019; Morales *et al.* 2018; Tanaka, Adachi & Yamori, 2019; Taylor & Long 2017; Wang, Burgess, de Becker & Long 2020; Zhu, Ort, Whitmarsh & Long 2004). The effects of non-steady-state conditions on

photosynthetic efficiency, including the effects of temporary shade, remain poorly characterised for a great many crop species.

Currently, a leading strategy for increasing crop efficiency is to improve radiation use efficiency (Ort *et al.* 2015; Zhu, Long & Ort 2010). A key area of progress is improving the speed at which photosynthesis responds to dynamic variation in sun and shade. Slow relaxation of non-photochemical quenching (NPQ) during sun-shade transitions is one factor that limits crop radiation use efficiency (Zhu *et al.* 2004), and speeding up this process has been shown to increase plant productivity (Kromdijk *et al.* 2016). Slow induction of photosynthesis during shade-sun transitions is also potentially important (Kaiser *et al.* 2015; Pearcy, Krall & Sassenrath-Cole 1996). Evidence suggests that slow induction significantly decreases diurnal CO₂ assimilation, and/or that there is significant genetic variation in rates of induction amenable to breeding in wheat (Salter, Merchant, Richards, Trethowan & Buckley 2019; Taylor & Long 2017), rice (Acevedo-Siaca *et al.* 2020; Yamori, Masumoto, Fukayama & Makino 2012), cassava (De Souza, Wang, Orr, Carmo-Silva & Long 2020), and soya (Soleh *et al.* 2016; Wang *et al.* 2020). However, dynamic changes in the components of non-stomatal limitations affecting photosynthesis during shade-sun transitions have been characterised infrequently, so it remains unclear whether interventions that target specific biochemical processes limiting induction of photosynthesis, e.g., increasing rates of Rubisco activation (Yamori *et al.* 2012), will be similarly effective in a broad range of crop species.

For C₃ leaves, supply of CO₂ mediated by stomatal conductance (Farquhar & Sharkey, 1982) results in net CO₂ assimilation rate (A)-intercellular [CO₂] (c_i) relationships (A/c_i responses) that are expected to be controlled by different biochemical limitations depending on c_i . At high light and lower c_i , photosynthesis is usually limited by maximum rates of RuBP carboxylation by Rubisco ($V_{c,max}$), but above a threshold c_i ($c_{i,trans}$) RuBP regeneration resulting from Calvin Benson Cycle turnover, driven principally by rates of

electron transport (J) becomes limiting (von Caemmerer & Farquhar 1981; Farquhar, von Caemmerer & Berry, 1980). Robert Pearcy and colleagues first extended this model to photosynthetic induction during the 1980s (reviewed in Pearcy *et al.* 1996), and their dynamic A/c_i method (Chazdon & Pearcy, 1986) remains a gold standard for analysing biochemical limitation during shade-sun transitions (Acevedo-Siaca *et al.* 2020; De Souza *et al.* 2020; Salter *et al.* 2019; Soleh *et al.* 2016; Taylor & Long, 2017). The dynamic A/c_i approach consists of a series of inductions measured at different $[\text{CO}_2]$ s. Early applications provided evidence that, subsequent to a 1-2 min RuBP-regeneration limited ‘fast-phase’ (Sassenrath-Cole & Pearcy 1992), slow increases in both $V_{c,\text{max}}$ and g_s are key controls affecting the rate at which A recovers following shade (Chazdon & Pearcy, 1986; Kirschbaum & Pearcy, 1988). This understanding facilitated subsequent work addressing the function of Rubisco activase (Rca), which drives increases in $V_{c,\text{max}}$ during induction (Carmo-Silva & Salvucci, 2013; Hammond, Andrews, Mott & Woodrow 1998; Woodrow & Mott, 1989), and the assumption of persistent $V_{c,\text{max}}$ limitation during induction has recently been used to improve methods for analysing biochemical and stomatal limitations during induction (Deans, Farquhar & Busch 2019a).

Despite their importance, a caveat of published dynamic A/c_i measurements is potential feedback between c_i and photosynthetic induction: greater c_i following shade is linked with faster induction (Kaiser, Kromdijk, Harbinson, Heuvelink & Marcelis, 2017; Kirschbaum & Pearcy 1988; Woodrow, Kelly & Mott 1996). Because this effect could inflate apparent rates of increase in $V_{c,\text{max}}$ obtained from dynamic A/c_i experiments, and underestimate absolute effects of $V_{c,\text{max}}$ on induction, alternative protocols that establish the dynamic behaviour of $V_{c,\text{max}}$ without holding leaves at different $[\text{CO}_2]$ s for extended periods can better establish impacts on crop performance.

The $[\text{CO}_2]$ denoting the transition from limitation by $V_{c,\text{max}}$ to limitation by J on the A/c_i response ($c_{i,\text{trans}}$) is an important parameter for understanding photosynthetic efficiency. Atmospheric $[\text{CO}_2]$ is higher today than at any stage since domestication of crop plants began (Indermühle *et al.* 1999; Larson *et al.* 2014; Sage 1995). Therefore, limitation by $V_{c,\text{max}}$ because of low c_i is likely to have been an important constraint on crop photosynthesis, including photosynthetic induction, throughout the history of agriculture. Today and in the future, however, higher ambient $[\text{CO}_2]$ and/or increasing nitrogen limitation (which diminishes $V_{c,\text{max}}$ and J) may result in more frequent limitation of A by J , including under saturating light conditions where $V_{c,\text{max}}$ would previously have been the primary biochemical control (Long, Ainsworth, Rogers & Ort 2004; Kromdijk & Long 2016). Whether the operating point for A falls at, or towards higher or lower c_i than $c_{i,\text{trans}}$, will impact photosynthetic optimisation and therefore efficiency of resource use under steady state conditions. Photosynthesis at or close to $c_{i,\text{trans}}$ implies balanced Calvin Benson Cycle function, maximizing returns on investment towards RuBP carboxylation and regeneration capacity (von Cammerer & Farquhar, 1981; Farquhar & Sharkey, 1982; Long *et al.* 2004; Kromdijk & Long 2016). Because the dynamic A/c_i method enables $c_{i,\text{trans}}$ to be determined under non-steady-state conditions (Taylor & Long 2017) and establishes the patterns and impacts of changes in $V_{c,\text{max}}$ and J , dynamic A/c_i measurements can provide unique mechanistic insights into deviations from optimal photosynthesis during induction.

Crops from the genus *Brassica* (L.) are key sources of vitamins and minerals globally (Rakow 2004) and provide interesting physiological contrasts. *Brassica* can differ considerably in terms of e.g., leaf size and thickness, and may be annual or biennial, which would be expected to drive alternative leaf structural and biochemical investments (Wright *et al.* 2004). The origins and inter-relationships between *Brassica* species are well understood (Liu *et al.* 2014; Parkin *et al.* 2005; Rana *et al.* 2004). From the perspective of understanding

how induction varies among crop accessions, the relationship between *B. oleracea* (L.), *B. rapa* (L.), and their allopolyploid hybrid *B. napus* (L.) is particularly interesting. Divergence between *B. oleracea* and *B. rapa* occurred as much as 4 Mya (Inaba & Nishio 2002), and *B. napus* most likely originated in agricultural settings, i.e., < 10 kya (Rana *et al.* 2004). Consequently, gene families from both *B. oleracea* and *B. rapa* that are present in the allopolyploid *B. napus* genome (Rana *et al.*, 2004), may include those specifying the small subunit of Rubisco and *Rca*. Their evolutionary history, therefore, makes these three species an interesting test of the extent to which fairly close relatives can show differentiation in non-steady-state photosynthesis, especially the impacts of $V_{c,max}$ on induction.

Using gas exchange and chlorophyll fluorescence, limitations affecting steady-state and non-steady-state photosynthesis were determined for *B. oleracea*, *B. napus* and *B. rapa*. 1) Steady-state leaf gas exchange was used in combination with biochemistry of leaf extracts to determine whether photosynthetic characteristics, including the predominant biochemical limitation, differed. 2) Gas exchange time-series for induction measured at ambient $[CO_2]$ were used to establish whether there were differences in terms of: fast- (before 2 min) and slow- (after 2 min) phases of induction, as well as periods dominated by non-stomatal factors, which include biochemistry (decreasing c_i), or effects of increasing g_s (increasing c_i). 3) Apparent biochemical limitations during induction were established in detail using a new dynamic A/c_i response methodology, designed to overcome a key caveat of previous experiments by not holding leaves at sub- or super-ambient $[CO_2]$ s for extended periods.

Materials and Methods

Plant material

The three *Brassica* were represented by: a commercial winter oil seed rape, *B. napus* cv. Elgar (Elsoms Seeds Ltd. Spalding, UK); Yellow Sarson, *B. rapa* ssp. *trilocularis* genotype

R-o-18, which has a similar developmental ontogeny to oilseed rape (Stephenson *et al.* 2010); and Gai lan, *B. oleracea* ssp. *alboglabra*, genotype A12DHd (R-o-18 and A12DHd, Warwick Crop Centre, Wellesbourne, UK).

Plants used for gas exchange measurements grew in controlled environment greenhouses set to maintain day/night temperatures at 24/18 °C. A 16 h daylength was maintained using supplementary lighting from high pressure sodium lamps (SON-T 400W, Philips Lighting, Eindhoven NL) that provided a photosynthetic photon flux density (PPFD) of $\sim 500 \mu\text{mol m}^{-2} \text{s}^{-1}$ at canopy level if external short-wave irradiance decreased below 250 W m^{-2} ($\sim 570 \mu\text{mol m}^{-2} \text{s}^{-1}$ PPFD). Seedlings were germinated in 40 mL cells (PG Mix, Yara, Grimsby, UK), and were transplanted to 1.5 L pots one week after emergence, in each case using a soil-less compost mix (Petersfield Products, Leicester, UK) that incorporated a broad range fertilizer. Checks were made daily to ensure that compost was kept moist without overwatering.

Plants used for biochemistry were also sown, germinated and transplanted to 1.5 L pots in the greenhouse, containing the same compost mix as above. They were then transferred into controlled environment cabinets (Microclima 1750, Snijders Scientific B.V., Netherlands) two weeks after transplanting. Cabinets were set to maintain day/night temperatures at 25/15 °C, RH was maintained at $\sim 60\%$, and a 16 h daylength was achieved with canopy-level PPFD $\sim 450 \mu\text{mol m}^{-2} \text{s}^{-1}$. Each species was sampled in five repeats of the experiment: four plants per species were transferred to the controlled environment cabinet, and after ~ 24 d in the cabinet, one leaf disc (0.55 cm^2) per plant was taken from the youngest fully expanded leaf and immediately snap frozen in liquid N_2 . To average out the effects of plant-to-plant variation, within each of the five batches of plants, the four discs per species were pooled for the Rubisco content and activity analyses described below.

Steady state photosynthesis

Measurements were made 5-6 weeks after planting for *B. rapa* and *B. napus*, and one or two weeks later for the slower growing *B. oleracea*. Recently expanded leaves were enclosed in the controlled environment cuvette of a photosynthesis system (LI-6800F, LI-COR, Lincoln NE, USA), which incorporates open-path infra-red CO₂ and H₂O analysers, and an integrated modulated fluorometer/light source. Leaf temperature was controlled at 25 °C, and leaf-air vapour pressure deficit (VPD_{leaf}) at 1.2 kPa. To measure photosynthetic responses to PPFD, leaves were brought to steady-state (stable *A* and stomatal conductance to water (*g_{sw}*) over 5 min) at a PPFD of 1500 μmol m⁻² s⁻¹ and [CO₂] of 392 ± 3.5 μmol mol⁻¹ (mean ± sd; reference channel 430 μmol mol⁻¹). PPFD was then varied to supply 2000, 1800, 1500, 1200, 1000, 800, 600, 500, 400, 300, 250, 200, 150, 100, 50, and 0 μmol m⁻² s⁻¹ inside the cuvette. Measurements were taken as soon as *A* stabilised at each PPFD. Leaves were brought back to steady-state under the initial conditions, then the steady-state response of *A* to *c_i* was determined using measurements at different reference CO₂ concentrations: firstly, 430, 300, 200, 150, 100, 50, and ~ 0 μmol mol⁻¹, then, after return to steady state at 430 μmol mol⁻¹; 500, 600, 700, 900, 1000, and 1200 μmol mol⁻¹. In addition to gas exchange parameters calculated following von Caemmerer and Farquhar (1981), measurements during CO₂ response curves captured steady state (*F_s*) and maximum (*F_m'*) fluorescence yields using a multiphase flash, allowing use of the effective quantum yield [$\Phi_{\text{PSII}} = (F_m' - F_s)/F_m'$] as an additional indicator of photosynthetic limitation-state based on its proportionality with *J* (e.g., Gu *et al.* 2010, Busch & Sage 2017; Supplementary Fig. 1).

Photosynthetic induction

Photosynthetic induction responses at ambient [CO₂] were measured by establishing steady-state gas exchange at: PPFD, 1500 μmol m⁻² s⁻¹; reference [CO₂], 430 μmol mol⁻¹; cuvette

air temperature, 25 °C; and cuvette RH 65% ($VPD_{\text{leaf}} 1.08 \pm 0.075$ kPa). A shade fleck was then simulated by a step decrease in PPFD to $150 \mu\text{mol m}^{-2} \text{s}^{-1}$ for 30 min, followed by a step increase back to $1500 \mu\text{mol m}^{-2} \text{s}^{-1}$. Gas analysers were matched one minute before starting the sun-shade-sun sequence, and measurements were logged every 10 s from one min before shade until at least 28 min after shade.

The following key timesteps from the 10 s resolution induction curves were identified. First, the end of the RuBP regeneration dominated ‘fast-phase’ of induction was taken to be 2 min after the return to high light, following shade. Second, $t_{c_i, \text{min}}$ was the time at which minimum c_i was observed during induction, marking the transition between predominant limitation by non-stomatal factors (which results in decreasing c_i) and increasing stomatal conductance (g_s ; which results in increasing c_i). Next, $t_{A,90}$ was the timepoint at which A had recovered 90% of the difference [A pre-shade – A end shade]. Using these timepoints, recovery in A , as a proportion of [A pre-shade – A shade], was attributed to the fast-phase (R_{fast}), non-stomatal dominated ($R_{c_i, \text{min}}$), and non-stomatal dominated recovery not attributable to the fast-phase ($R_{c_i, \text{min}} - R_{\text{fast}}$), i.e., slow phase non-stomatal recovery. The duration of recovery dominated by effects of g_s was approximated by $t_{A,90} - t_{c_i, \text{min}}$.

Dynamic A/c_i measurements

To characterise changes in factors limiting photosynthesis during shade-sun transitions, a dynamic A/c_i method was implemented that improved on previously published versions (Acevedo-Siaca *et al.* 2020; Chazdon & Pearcy 1986; De Souza *et al.* 2020; Salter *et al.* 2019; Soleh *et al.* 2016; Taylor & Long 2017) by removing the potentially confounding effect of extended incubation in various [CO_2]_s. Leaves were first brought to steady state under the same conditions as for measurements of photosynthetic induction described above. A 30 min period of shade was then imposed using a PPFD of $100 \mu\text{mol m}^{-2} \text{s}^{-1}$. Following

Taylor & Long (2017), to prevent stomatal closure in response to this shade by maintaining c_i at approximately twice the compensation point (spot measurements prior to end of shade period: mean \pm sd, $93 \pm 1.3 \mu\text{mol mol}^{-1}$, $N = 328$ inductions), reference $[\text{CO}_2]$ was controlled at $100 \mu\text{mol mol}^{-1}$ during the shade. At the end of 30 min shade, PPFD was returned to its initial value of $1500 \mu\text{mol m}^{-2} \text{s}^{-1}$ and $[\text{CO}_2]$ was set to the first of a stratified random sequence of ten $[\text{CO}_2]$ s, measured at two min intervals so that chamber stability and IRGA matching could be achieved reliably. For each leaf to be measured, an independent sequence of reference $[\text{CO}_2]$ s was drawn from the following set: 50, 100, 200, 300, 400, 500, 600, 700, 800, and $1000 \mu\text{mol mol}^{-1}$. The $[\text{CO}_2]$ s were ordered so that concentrations from the $\leq 400 \mu\text{mol mol}^{-1}$ and $\geq 500 \mu\text{mol mol}^{-1}$ ranges were interspersed randomly (e.g., 800, 200, 600, 100, 500, 400, 700, 300, 1000, 50), and were rotated over ten separate inductions so that every $[\text{CO}_2]$ was measured at every interval between 2 and 20 min following shade (Supplementary Fig. 2). To aid with consistency of responses, measurements were made in the laboratory (i.e., low light, and relatively constant temperature and humidity conditions), and between inductions gas exchange was allowed to fully recover to steady state at reference $[\text{CO}_2]$ of $430 \mu\text{mol mol}^{-1}$. To ensure that induction measurements for a leaf could be captured within a single day, two LI-6800F were used, attached adjacent to one another, either side of the mid-rib.

Models

The relationship between A and incident PPFD was modelled as a non-rectangular hyperbola (Long & Hallgren 1985):

$$A = \frac{\phi I + A_{\text{sat}} - \sqrt{(\phi I + A_{\text{sat}})^2 - 4\theta\phi I A_{\text{sat}}}}{2\theta} - R_d$$

Where: ϕ is the apparent quantum yield (mol mol^{-1}); I , incident PPFD ($\mu\text{mol m}^{-2} \text{s}^{-1}$); A_{sat} , the maximum gross rate of leaf CO_2 assimilation ($\mu\text{mol m}^{-2} \text{s}^{-1}$); θ , a dimensionless curvature parameter; and R_d , day respiration ($\mu\text{mol m}^{-2} \text{s}^{-1}$).

With values for $[\text{CO}_2]$ in partial pressure units, the FvCB model (von Caemmerer & Farquhar 1981; Farquhar *et al.* 1980) was used to characterise A/c_i relationships:

$$A = \min(W_C, W_J, W_P)(1 - \Gamma^*/c_c) - R_d$$

$$W_C = V_{c,\text{max}}c_c/(c_c + K_{\text{CO}})$$

$$W_J = Jc_c/(4c_c + 8\Gamma^*)$$

$$W_P = 3T_P c_c/(c_c - \Gamma^*)$$

where W_C is the Rubisco limited, W_J electron transport limited, and W_P triose-phosphate utilisation limited rate of carboxylation. The $[\text{CO}_2]$ at the site of carboxylation in the chloroplast, $c_c = c_i - A/g_m$. Additional parameters are: Γ^* , the photosynthetic CO_2 compensation point in the absence of R_d ; $V_{c,\text{max}}$, the maximum carboxylation rate of Rubisco; $K_{\text{CO}} = K_C(1+O/K_O)$, where K_C and K_O are the respective Michaelis constants for Rubisco catalysis of carboxylation and oxygenation reactions, and O is the partial pressure of O_2 ; J , electron transport rate; T_P , the rate of triose phosphate utilisation.

To identify the match between c_i and W_C , W_J , and W_P as limiting factors we used the approach of Gu, Pallardy, Tu, Law & Wullschleger (2010), fitting values for $V_{c,\text{max}}$, J , and T_P using:

$$A = \frac{b - \sqrt{b^2 - 4c}}{2}$$

For A_C :

$$b = V_{c,\text{max}} - R_d + g_m(c_i + K_{\text{CO}})$$

$$c = g_m(V_{c,\text{max}}(c_i - \Gamma^*) - R_d(c_i + K_{\text{CO}}))$$

For A_J :

$$b = J/4 - R_d + g_m(c_i + 2\Gamma^*)$$

$$c = g_m(J/4(c_i - \Gamma^*) - R_d(c_i + 2\Gamma^*))$$

For A_P :

$$b = 3T_p - R_d + g_m(c_i - \Gamma^*)$$

$$c = g_m(3T_p(c_i - \Gamma^*) - R_d(c_i - \Gamma^*))$$

For each A/c_i response, all possible limitation-state combinations were tested, given the required order of limitation states along the c_i axis ($W_C < W_J < W_P$), and the minimum number of data necessary for each limitation state ($N \geq 2$ when K_{CO} and Γ^* are fixed). The R Language and Environment function *optim* (R Core Team 2018) was used to minimise the distribution-wise cost function, accepting the model with the lowest value after checking for admissibility and testing for co-limited ‘swinging points’ (Gu *et al.* 2010).

Using this method, estimation of g_m from the data was found not to credibly predict limitation states indicated by Φ_{PSII} (e.g., Busch & Sage 2017), so for consistency g_m was assumed to be infinite throughout (approximated by setting g_m to $1 \times 10^6 \mu\text{mol m}^{-2} \text{s}^{-1} \text{Pa}^{-1}$). Values for $V_{c,\text{max}}$, J and T_p are thus apparent rates, and in the dynamic A/c_i analysis are confounded with any dynamic variation in g_m . Similarly, to ensure credible values, mean leaf temperatures measured in the LI-6800F were used to predict Γ^* , K_C and K_O , using values for tobacco (Sharkey, Bernacchi, Farquhar & Singsaas 2007). Combining the Sharkey *et al.* (2007) coefficients with estimation of R_d as part of the fitting process provided the best fit in the region around Γ^* for parameterisation of steady-state responses (for comparisons among parameterisations, see Supplementary Fig. 3).

In the dynamic A/c_i analysis, where greater measurement error and a slightly reduced number of measurements made least-squares fits less reliable, genotype-level parameters from the steady-state A/c_i measurements were used to ensure A/c_i fits provided a reasonably close match with limitation states indicated by Φ_{PSII} (Supplementary Fig. 2). The value of R_d

was fixed. In addition, A_p was initially assigned only to points with $c_i \geq$ that at which limitation transitioned from J to T_p in the steady-state. If best-fit, admissible models predicted T_p , they were only accepted if they also predicted $V_{c,max}$ and J , otherwise data assigned to A_p were dropped and the model was refit, dropping the highest c_i data as necessary until a best-fit admissible model was found that either (a) included both A_C and A_J , or (b) included A_C alone. When a best fit model with A_C alone was reached, because identification of A_J requires $N \geq 2$, the uppermost c_i value was dropped to prevent mis-attribution of data that could be assigned to A_J and the model was refit, taking the highest c_i used as a lower-bound value for $c_{i,trans}$.

Stomatal limitation (L_S) was calculated from the steady-state A/c_i responses following Farquhar & Sharkey (1982):

$$L_S = \frac{A_0 - A}{A_0}$$

Where, A_0 is a reference net CO_2 assimilation rate predicted at a c_i equal to leaf external $[CO_2]$, and A was the rate observed at the initial reference $[CO_2]$ of $430 \mu\text{mol mol}^{-1}$.

Analyses of Rubisco activity, and content of Rubisco, total soluble protein, and chlorophylls

Leaf samples consisting of four leaf discs (2.2 cm^2 per sample) were homogenised in 0.6 mL of extraction buffer (50 mM Bicine-NaOH pH 8.2, 20 mM $MgCl_2$, 1 mM EDTA, 2 mM benzamidine, 5 mM ϵ -aminocaproic acid, 50 mM 2-mercaptoethanol, 10 mM dithiothreitol, 1% (v/v) protease inhibitor cocktail (Sigma-Aldrich, Mo, USA), and 1 mM phenylmethylsulphonyl fluoride) using an ice-cold mortar and pestle. Rapid grinding ($< 60 \text{ s}$) was followed by centrifugation of the homogenate at $4 \text{ }^\circ\text{C}$, 21000 g for 1 min. The supernatant was collected and used to determine Rubisco total activity by $^{14}CO_2$ incorporation into acid-stable products as described previously (Carmo-Silva *et al.* 2017).

The supernatant (20 mm^3) was incubated for 3 min in 500 mm^3 of reaction mixture (100 mM

Bicine-NaOH pH 8.2, 20 mM MgCl₂, 10 mM NaH¹⁴CO₂ [9.25 kBq μmol⁻¹], and 2 mM KH₂PO₄) to fully carbamylate Rubisco. RuBP was then added (to 0.6 mM) to initiate the reaction, and assays quenched with 10 M formic acid after 30 s. Reaction mixtures were dried, the residue re-suspended, and scintillation counted as described previously (De Souza, *et al.* 2020). The same supernatant was used to determine Rubisco content by mixing 100 mm³ of supernatant with 100 mm³ of CABP binding buffer (100 mM Bicine-NaOH pH 8.2, 20 mM MgCl₂, 20 mM NaHCO₃, 1.2 mM [¹⁴C]CABP [carboxyarabinitol-1,5-bisphosphate, 37 kBq μmol⁻¹]), incubating at ~ 20 °C for 30 min, then following the column-based [¹⁴C]CABP binding assay described previously (Sharwood, Sonawane, Ghannoum & Whitney 2016).

Total soluble protein (TSP) was determined for aliquots taken from the supernatant used for Rubisco analyses via Bradford assay (Bradford 1976). Chlorophyll content was determined from an aliquot of the leaf homogenates prior to centrifugation, which was added to ethanol (Wintermans & de Mots 1965). Absorbance for TSP and chlorophyll determinations was measured in a SPECTROstar Nano microplate reader (BMG LabTech, Aylesbury, UK).

Statistical analyses

Modelling and statistical analyses were carried out using R Language and Environment 3.5.2 (R Core Team 2018). Among species differences were tested using one-way anova and Tukey's Honest Significant Difference, and the homogeneity assumption was validated using Bartlett's test.

For parameters from dynamic A/c_i analysis, generalised additive mixed models (GAMM, package *mgcv* version 1.8-26) were used to summarize time-dependent changes without the need to assume particular underlying mechanisms. When fitting GAMM,

Brassica species were treated as fixed effects, allowing unique species-level functions with respect to time. Independently measured plants were treated as random effects influencing variance around the species-level functions (Zuur, Ieno, Walker, Saveliev & G M Smith 2009). The slopes of fitted functions for $V_{c,max}$ against time ($dV_{c,max}/dt$) from dynamic A/c_i were obtained by finite differencing from values predicted by GAMM at 1 s resolution. Species specific confidence intervals for GAMM were approximated as: predicted values $\pm t_{1-\alpha,edf} \times SEM$, where $\alpha = 0.025$, and edf = estimated degrees of freedom at the species level.

Results

Steady state photosynthesis and biochemical characteristics

Photosynthetic response to light and leaf biochemistry

Leaf level responses to PPF (Fig. 1) showed mean values of A_{sat} , R_d , and θ that were highest for *B. rapa*, slightly lower for *B. napus*, and lowest for *B. oleracea* (Fig. 1). By contrast, ϕ was greater in *B. oleracea* and *B. napus* than in *B. rapa*. There was limited support for significant differences in R_d ($F_{2,9} = 2.22$, $P = 0.16$) and ϕ ($F_{2,9} = 2.56$, $P = 0.13$) across the three *Brassica*. However, differences in A_{sat} were marginally significant ($F_{2,9} = 3.03$, $P = 0.099$), and there was strong evidence for a significant difference in θ ($F_{2,9} = 9.91$, $P = 0.005$). The smaller θ for *B. oleracea* compared with *B. napus* and *B. rapa*, supports a more gradual transition from light- to carboxylation-limited photosynthesis at higher PPFs and was significant for both individual comparisons ($P \leq 0.026$).

The observed patterns of differences in mean Rubisco total activity and Rubisco amount were consistent with marginally significant differences in mean A_{sat} . Rubisco amount and total activity were lower in *B. oleracea* than in *B. napus* and *B. rapa* (Table 1), though these differences were not significant among the three species ($F_{2,12} \leq 1.6$, $P \geq 0.24$). Normalised to Rubisco content, Rubisco specific activities were even more similar than total

activities among the three *Brassica* (Table 1), implying that patterns of difference in total activity were strongly affected by amounts of Rubisco protein per unit leaf area. Interestingly, while the lower Rubisco content of *B. oleracea* leaves was paired with similar total soluble protein to *B. rapa* ($P = 0.94$), these two species showed marked differences in chlorophylls. *B. oleracea* had approximately double the amount of chlorophyll a+b ($P < 0.001$), and lower chlorophyll a:b ratios ($P = 0.001$) compared with *B. rapa* (Table 1). By contrast, *B. napus* had higher soluble protein content compared with the other two *Brassica* ($P \leq 0.029$; Table 1), intermediate chlorophyll content (*B. napus*-*B. oleracea*, $P = 0.084$; *B. napus*-*B. rapa*, $P = 0.002$) and intermediate chlorophyll a:b ratio (*B. napus*-*B. oleracea*, $P = 0.089$; *B. napus*-*B. rapa*, $P = 0.089$). Thus, while Rubisco content was aligned with A_{sat} , it was opposite to investments in chlorophyll pigments, which were significantly less in leaves of *B. rapa* compared with *B. oleracea*.

Photosynthetic response to CO₂

Operating point A and g_{sw} were significantly lower for *B. oleracea* than for *B. rapa* (A , $P = 0.021$; g_{sw} , $P = 0.017$). For both A and g_{sw} , *B. napus* was intermediate between the other *Brassica*: there was a marginally significant difference in A between *B. napus* and *B. oleracea* ($P = 0.064$); little support for a significant difference in g_{sw} between them ($P = 0.15$); and no significant difference in either A or g_{sw} between *B. napus* and *B. rapa* ($P \geq 0.31$; Table 2). The significant differences between A and g_{sw} of *B. oleracea* and *B. rapa* were associated with an increase in mean c_i from 26.5 (*B. oleracea*) to 29.3 Pa (*B. rapa*), but measurements were not sufficiently repeatable across the small number of replicates to establish a significant difference in c_i among the three species ($F_{2,9} = 2.56$, $P = 0.13$; Table 1).

The similarity in operating c_i , and differences in A and g_{sw} between the *Brassica* were associated with differences in steady state A/c_i responses (Fig. 2; Supplementary Fig. 1).

Mean $V_{c,max}$ and J were, as for A , highest in $B. rapa$, intermediate in $B. napus$, and lowest in $B. oleracea$. While the three primary rate limiting factors: $V_{c,max}$, J and T_p , were not significantly different between the three *Brassica* ($F_{2,9} \leq 2.16$, $P \geq 0.17$; Fig. 2), differences in L_S were ($F_{2,9} = 5.01$, $P = 0.035$), specifically between $B. rapa$ and $B. oleracea$ ($P = 0.037$, other comparisons $P \geq 0.089$; Table 2). There was also a marginally significant difference in $c_{i,trans}$ ($F_{2,9} = 4.1$, $P = 0.054$), with $B. oleracea$ showing the highest $c_{i,trans}$ and $B. rapa$ the lowest: the range of c_i that is expected to result in $V_{c,max}$ limiting A was significantly greater for $B. oleracea$ than $B. rapa$. In combination, small differences in $V_{c,max}$, J , and g_s led to operating c_i that was significantly lower than $c_{i,trans}$ in $B. oleracea$ (one tailed, paired t-test: $t_3 = 3.61$, $P = 0.005$), but overlapped with $c_{i,trans}$ in $B. napus$ and $B. rapa$ (two tailed, paired t-test: $t_3 < \pm 1.69$, $P \geq 0.19$). Thus, in the steady state, carboxylation in leaves of $B. oleracea$ was limited by $V_{c,max}$, whereas $B. napus$ and $B. rapa$ operated at the transition between $V_{c,max}$ and J limitation (Fig. 2; Supplementary Fig. 1). Finally, though at much higher c_i than the operating point, a highly significant difference was also shown for the c_i at which A_J transitioned to A_P ($F_{2,9} = 10.38$, $P = 0.006$), between $B. napus$, which had the lowest value for the c_i of this transition, and $B. oleracea$, which had the highest (Fig. 2; $P = 0.005$).

Photosynthetic induction

Recovery of A during fast, mesophyll-dominated, and stomata-limited induction

The vast majority of recovery in A occurred while c_i was decreasing, i.e., while recovery of A was controlled primarily by non-stomatal factors (Fig. 3); recovery of A during this 4-5 min period ($t_{ci,min}$, Table 3) averaged 77-84% ($R_{ci,min}$, Table 3). After 30 min shade at the relatively high shade-irradiance of $150 \mu\text{mol m}^{-2} \text{s}^{-1}$, ~ 70% of recovery occurred during the first 2 min (fast-phase), so slow-phase recovery prior to increases in c_i accounted for ~ 10% of the shade-sun difference in A (Table 3). When the fast- and slow-phase components of

non-stomatal-dominated recovery were taken together, neither their combined impact on recovery of A nor their combined duration were significantly different between the three *Brassica* ($R_{c_i, \min}$, $P = 0.51$; $t_{c_i, \min}$, $P = 0.24$).

By contrast with non-stomatal-dominated induction, the remaining 20% of recovery in A , that was predominated by the effect of increasing g_s on c_i , took significantly longer in *B. oleracea* than in *B. rapa* ($t_{A,90} - t_{c_i, \min}$, Table 3; $P = 0.02$), and was marginally significantly longer in *B. oleracea* than *B. napus* (Tukey HSD, $P = 0.055$; Table 3). Mean A , g_{sw} and c_i of *B. oleracea* had not approached their steady-state values even after 20 min of induction (Fig. 4a), such that $t_{A,90}$ was significantly longer in *B. oleracea* than the other two species (Table 3; $F_{2,9} = 7.24$, $P = 0.013$; *B. oleracea*-*B. napus*, $P = 0.034$; *B. oleracea*-*B. rapa*, $P = 0.017$). Contrasting with *B. oleracea*, both *B. napus* and *B. rapa* reached $t_{A,90}$ within 10 min induction (Table 3), even though, like *B. oleracea*, their g_{sw} and c_i continued to increase beyond 20 min, A was insensitive to this (Fig. 3 and 5).

Apparent limiting biochemical factors during induction - dynamic A/c_i

Progressive changes in $V_{c, \max}$ determined from dynamic A/c_i responses were qualitatively different between the three *Brassica* (Fig. 4). Increases in $V_{c, \max}$ during induction were: 23% in *B. oleracea*, 33% in *B. napus* and 29% in *B. rapa*. The rate of change in $V_{c, \max}$ ($dV_{c, \max}/dt$) declined smoothly (Fig. 4d), and confirmed that increases in $V_{c, \max}$ were predominantly over the first ~ 10 min of induction in *B. oleracea*, ~ 12 min in *B. rapa* (Fig. 4a, c & d), and ~18 min in *B. napus* (Fig. 4b & d). In all three, $V_{c, \max}$ increased rapidly for the first 4-5 min of induction, coinciding with the $t_{c_i, \min}$ observed in induction measurements (Table 3). It was also notable that $V_{c, \max}$ of *B. oleracea* saturated before $t_{A,90}$ from the ambient induction experiments, whereas increases in $V_{c, \max}$ of *B. napus* and *B. rapa* were continuing at their $t_{A,90}$, but with little subsequent effect on A (Fig. 4).

The c_i at which limitation transitioned away from $V_{c,\max}(c_{i,\text{trans}})$, which is co-determined by $V_{c,\max}$ and J , was initially similar to ambient $[\text{CO}_2]$ and decreased during induction. After 4-6 min induction, $c_{i,\text{trans}}$ was indistinguishable from steady-state values on the basis of approximate 95% confidence intervals (Fig. 5). Comparing time series for $c_{i,\text{trans}}$ (shade PPF, $100 \mu\text{mol mol}^{-1}$) with c_i during induction at ambient $[\text{CO}_2]$ (shade PPF $150 \mu\text{mol m}^{-2} \text{s}^{-1}$; Fig. 5), by 20 min their values were essentially the same as those found at steady-state (i.e. *B. oleracea*, $c_i < c_{i,\text{trans}}$; *B. napus*, $c_i \sim c_{i,\text{trans}}$; *B. rapa* $c_i \sim c_{i,\text{trans}}$). Based on 95% confidence intervals, c_i was significantly less than $c_{i,\text{trans}}$ throughout induction for *B. oleracea* (Fig. 5a), until ~ 10 min for *B. napus* (Fig. 5b), and until ~ 7 min in *B. rapa* (Fig. 5c), with c_i intersecting mean $c_{i,\text{trans}}$ after 10-15 min induction in *B. napus* and *B. rapa*. Because $c_i < c_{i,\text{trans}}$ infers that A is limited by $V_{c,\max}$, as $c_i < c_{i,\text{trans}}$ throughout induction A of *B. oleracea* was always $V_{c,\max}$ -limited, and the other two species were $V_{c,\max}$ limited beyond $t_{A,90}$ (Table 3). Because $c_{i,\text{trans}}$ denotes a change in the slope of the A/c_i response, overlap between $c_{i,\text{trans}}$ and c_i of *B. napus* and *B. rapa* during induction explains why A saturated while their g_s and c_i continued to increase (Fig 3b & c).

Discussion

Photosynthesis differed in several ways between *B. rapa* and *B. oleracea*. Most notably, the former had greater rates of gas exchange and recovered steady-state A more rapidly following shade. *B. napus* was intermediate in most respects, although more similar to *B. rapa*. A novel dynamic A/c_i response protocol that added randomisation of $[\text{CO}_2]$ s during induction to a previous innovation of fixed low $[\text{CO}_2]$ during shade (Taylor & Long 2017), imposed robust control for $[\text{CO}_2]$ during induction. The dynamic A/c_i experiments demonstrated that all three *Brassica* were limited by apparent $V_{c,\max}$ for 10 min or more following 30 min shade. Importantly though, while *B. oleracea* stayed $V_{c,\max}$ limited, *B. napus* and *B. rapa* transitioned

to co-limitation by J after ~ 10 min. The transitions to co-limitation coincided broadly with saturation of A , explaining why ongoing increases in g_s and/or $V_{c,max}$ had little subsequent effect in these two species, and providing a potential mechanistic explanation for previous observations of diversity among species in rates of recovery of A relative to g_s (Deans, Brodribb, Busch & Farquhar 2019b; McAusland *et al.* 2016).

Limitations affecting steady-state photosynthesis

The difference in limitation-states affecting steady-state A of the three species was not an anticipated outcome, but was clear. All three operated within 5 Pa of their $c_{i,trans}$. This is consistent with the hypothesis that operation close to $c_{i,trans}$ reflects optimisation of resource investment between capacities for carboxylation and RuBP regeneration (von Caemmerer & Farquhar 1981; Farquhar & Sharkey 1982), and perhaps indicative of acclimation to recent rapid increases in atmospheric $[CO_2]$ (Long *et al.* 2004; Kromdijk & Long 2016).

The amount of Rubisco and its total activity were a match for species differences in apparent $V_{c,max}$ and a better explanation of $V_{c,max}$ than differences in Rubisco performance. All three *Brassica* had similar Rubisco specific activities. Compared with Rubisco properties, differences in chlorophyll and total soluble protein were more easily detected. *B. oleracea* had double the chlorophyll a+b content compared with *B. rapa*, and the leaves of *B. oleracea* showed a more gradual transition away from light limitation as PPFD increased (significantly lower θ). *B. oleracea* A12DHd had particularly thick, noticeably waxy leaves and may experience limited light saturation deeper in the mesophyll (Hikosaka & Terashima 1995), especially when using the red/blue light source of the LI-6800F (Terashima *et al.* 2009). Reflectance from the waxy leaf surface may also reduce absorption by *B. oleracea* leaves and the species had lower chlorophyll a:b indicating a greater proportion of light harvesting chlorophylls, consistent with shade adaptation within the leaf. Evidence from biochemistry

and light response curves is therefore consistent with linkages between different steady-state photosynthetic limitations in these *Brassica* and higher-level structural differences.

Limitation of A by apparent $V_{c,max}$ in *B. oleracea* was clearly linked with lower g_s and greater L_S than in *B. napus* and *B. rapa*. The other key component of diffusive limitation affecting photosynthesis, g_m , was not reliably estimated with our data using exhaustive dual optimisation. To obtain consistent visual matching between predicted limitation states and the inflexion of both A/c_i and Φ_{PSII} in our three-species dataset required an effectively infinite value for g_m . However, the modified exhaustive dual optimisation approach (Gu *et al.* 2010) is a powerful tool for identifying $c_{i,trans}$ based on the inflexion of the A/c_i response, and incorporating a finite value for g_m in the model of photosynthesis does not affect whether operating point A falls above or below this inflexion.

Adequate fits for A/c_i responses in the region of Γ^* were achieved using the tobacco-derived parameterisation of Sharkey *et al.* (2007). By contrast, estimates of Rubisco kinetic parameters for *B. oleracea* reported in the literature (Hermida-Carrera, Kapralov & Galmés 2016) provided poor fits in this region (Supplementary Fig. 3). Compared with coefficients based on gas exchange measurements using tobacco (Sharkey *et al.* 2007), values for *B. oleracea* determined using *in vitro* measurements (Hermida-Carrera *et al.* 2016) are 7.5 Pa less for K_{CO_2} , and 0.8 Pa greater for Γ^* . As a consequence, Rubisco kinetic properties from Hermida-Carrera *et al.* (2016) predicted $V_{c,max}$ to be ~ 6% greater; however, their Γ^* exceeded the CO_2 compensation points we measured in all three *Brassica* (Supplementary Fig. 3). While the parameterisation we used for g_m means that the reported biochemical rates of $V_{c,max}$ and J incorporate differences in mesophyll properties, the fact that total activity of Rubisco from leaf extracts scaled with values for $V_{c,max}$ strongly corroborates the finding of lower $V_{c,max}$ in *B. oleracea*. Irrespective of the differences between published kinetic coefficients, therefore, *B. oleracea* had lower $V_{c,max}$ and was $V_{c,max}$ limited over a greater

range of c_i than the other two species. Increasing Rubisco activity (e.g., Salesse-Smith, Sharwood, Busch, Kromdijk, Bardal & Stern 2018; Yoon *et al.* 2020) could be particularly useful for improvement of photosynthesis in *B. oleracea*, assuming the genotype tested here is representative of the species.

Components of recovery in A during induction.

In all three *Brassica*, in addition to 70% of recovery attributable to fast-phase RuBP regeneration, and prior to increases in c_i and A linked with increasing g_s , slow-phase induction was initially dominated by non-stomatal effects consistent with Rubisco activation, which accounted for at least 10% of recovery in A . This fairly small value probably arose because of the relatively high PPFD ($150 \mu\text{mol m}^{-2} \text{s}^{-1}$) used during shade, and the fact that steady-state g_s was obtained in saturating light prior to imposing shade, hence relatively high g_s at the start of induction (Kirschbaum & Pearcy 1988). Use of relatively high shade PPFD and pre-acclimation to saturating light makes our measurements most relevant to midday photosynthesis in upper layers of crop canopies (Burgess *et al.* 2016; Townsend *et al.* 2018; Zhu *et al.* 2004). In situations where initial $V_{c,\text{max}}$ and/or g_s are lower, e.g., deeper layers of crop canopies where sunlit periods are interspersed by longer shade periods or preceded by persistent low light, more extended and larger impacts of $V_{c,\text{max}}$ would be expected when leaves are sunlit (Morales *et al.* 2018). The relatively high PPFD used here during shade also ensured that stomata remained the predominant route of water loss throughout our experiments, decreasing the risk of errors in calculated c_i (Hanson, Stutz & Boyer 2016) and enabling use of c_i as a sensitive indicator of whether mesophyll or diffusive factors were the predominant control over A .

The initial decrease in c_i always extended to ~ 4 -5 min of induction, at least twice the 2 min assumed to mark the end of the RuBP-regeneration dominated fast-phase. The 2 min

upper limit for the fast-phase is taken from the literature (e.g., Sassenrath-Cole & Pearcy 1992), and was used because gas exchange system mixing times meant that fast-phase kinetics could not be directly parameterised. The inflection of A indicating the end of the fast phase nonetheless tended to occur slightly before 2 min (e.g., Fig. 3), so the estimate of photosynthetic recovery driven by Rubisco activation, at 2-3 min duration and 10%, is conservative. Evidence that shade-induced Rubisco deactivation can limit midday photosynthesis in field crops is consistent with previous detailed measurements of apparent $V_{c,max}$ following sun-shade-sun transitions in wheat (Taylor & Long 2017; Salter *et al.* 2019), and experiments that manipulated Rca in rice (Yamori *et al.* 2012).

Beginning after 4-5 min of induction, increasing g_s outweighed non-stomatal components as a determinant of increasing c_i and A . At this time $c_{i,trans}$ was very close to its steady-state value. Despite the similar timing of transitions to g_s -dominated induction, recovery in A was less strongly and persistently affected by g_s in *B. napus* and *B. rapa* than *B. oleracea*. This might suggest that the prediction of Morales *et al.* (2018), based on careful reconstruction of photosynthetic regulation in Arabidopsis, that persistent stomatal limitation should be observed during longer light flecks, is not general across close crop relatives. There is evidence for considerable variation among plants, including different functional types, in the extent of stomatal limitation during induction (Deans, Brodribb, Busch & Farquhar 2019b; McAusland *et al.* 2016). Intraspecific studies addressing crops have also confirmed that the importance of stomatal limitations during induction can differ between species: stomata have little apparent importance in determining genetic variation for induction in soybean or rice (Acevedo-Siaca *et al.* 2020; Soleh *et al.* 2016), but are a dominant factor in cassava (De Souza *et al.* 2020).

Biochemical limitation-states during induction

To evaluate dynamic changes in $V_{c,max}$ and Rubisco limitation *in planta* requires dynamic A/c_i response measurements (Chazdon & Pearcy 1986; Salter et al., 2019; Soleh *et al.* 2016; Taylor & Long 2017). To avoid the potential caveat of $[CO_2]$ effects on half times for photosynthetic induction (Kaiser *et al.* 2017; Woodrow *et al.* 1996), the new dynamic A/c_i protocol used here varied $[CO_2]$ during every induction. This increased the interval between measurements to 2 min compared with 10 s in previous studies (Salter *et al.* 2019; Soleh *et al.* 2016; Taylor & Long 2017), so half times for apparent $V_{c,max}$ based on exponential curve fitting (Salter *et al.* 2019; Taylor & Long 2017) were less reliable and we analysed time series using GAMM. Though more qualitative, this analysis provided evidence that increases in apparent $V_{c,max}$ of *B. napus* are sustained over longer periods than in the other two; it augmented the traditional perspective of a two-phase RuBP regeneration and Rubisco activation limited sequence (Pearcy *et al.* 1996) by providing evidence for transitions to co-limitation by J after ~ 10 min of induction in *B. napus* and *B. rapa*; and it correctly reproduced limitation-states observed in steady-state measurements 20 min into induction.

As with induction experiments, recovery of apparent $V_{c,max}$ was evaluated following shade treatments consistent with expectations for field crops (Burgess *et al.* 2016; Townsend *et al.* 2018; Zhu, Ort, Whitmarsh & Long 2004). The relatively high PPFD used to simulate shade may explain the smaller increases in $V_{c,max}$ (23-33% compared with $> \sim 40\%$) than were observed in sun-shade-sun experiments with wheat (Salter *et al.* 2019; Taylor & Long 2017). Timescales for increases in apparent $V_{c,max}$ were, however, consistent with those of wheat, i.e., saturating after 10-15 min induction. That apparent $V_{c,max}$ continued to increase after $t_{ci,min}$ agrees with results from both dynamic A/c_i (Chazdon & Pearcy 1986) and A^* (c_i -corrected A , Woodrow & Mott 1989) methods used to establish the duration and impacts of

slow-phase limitations. Our results therefore validate the use of those values to model impacts of Rubisco activation during induction (Morales *et al.* 2018; Wang *et al.* 2020).

As c_i increased during induction, after ~ 10 min it began to coincide with and exceed $c_{i,trans}$ of both *B. napus* and *B. rapa*. This experimental outcome has important consequences for both the simplified A^* approach to evaluation of biochemical limitations (Woodrow & Mott 1989; Hammond *et al.* 1998) and a recent method incorporating more detailed models of leaf gas exchange to quantify stomatal limitation based on more realistic assumptions about the shape of the A/c_i response (Deans *et al.* 2019a). Both methods assume Rubisco limitation, and our results suggest this is valid in broad terms, but the methods will suffer from reduced accuracy if and when c_i approaches $c_{i,trans}$, because $c_{i,trans}$ marks an inflection in the response of A to c_i .

Persistent $V_{c,max}$ limitation in *B. oleracea* meant that A continued to respond to changes in both $V_{c,max}$ and g_s even after 20 min induction. By contrast, transitions to co-limitation by J after ~ 10 min induction in *B. napus* and *B. rapa*, meant A subsequently showed decreased sensitivity to changing $V_{c,max}$ and g_s . *B. napus* and *B. rapa* therefore overcame the effects of shade on A more rapidly. Because $c_{i,trans}$ marks an inflection in the response of A to g_s , it has been argued that steady-state operating points in the vicinity of $c_{i,trans}$ can encompass a wide range of values for the marginal cost of water use ($\delta E/\delta A$; von Caemmerer & Farquhar 1981; Farquhar & Sharkey 1982), compatible with a range of alternative water use strategies (Cowan & Farquhar, 1977; Cowan, 1982). An alternative view might be that operation close to $c_{i,trans}$, as observed for *B. napus* and *B. rapa*, results in more rapid declines in A/g_{sw} (intrinsic water use efficiency) during induction, compared with $c_i < c_{i,trans}$, i.e., persistent Rubisco limitation as in *B. oleracea*. Do faster photosynthetic responses to shade among crop plants trade-off against regulation of leaf water status? Further characterisation of the temporal characteristics and/or frequency of deviations

between c_i and $c_{i,\text{trans}}$ using dynamic A/c_i might provide useful insights into trade-offs between optimisation of radiation and water use efficiencies.

Conclusions

Measurements of three agriculturally important *Brassica* showed that in addition to classic fast RuBP regeneration and slow $V_{c,\text{max}}$ limited phases, transitions to co-limitation by J affect the dynamics of photosynthesis following shade. In leaves where c_i approached $c_{i,\text{trans}}$ more quickly during induction, subsequent photosynthesis was less sensitive to ongoing changes in $V_{c,\text{max}}$ and g_s . Diurnal productivity of C_3 crops with lower $c_{i,\text{trans}}$ would therefore be expected to be less sensitive to shade. Finally, although only one genotype of each crop was examined, these crops can be interbred, and the variation identified here shows scope for physiologically guided breeding to achieve improved photosynthetic efficiency.

Acknowledgements

This work was supported by Lancaster University, and by a subaward from the University of Illinois as part of the research project Realizing Increased Photosynthetic Efficiency (RIPE) that is funded by the Bill & Melinda Gates Foundation, Foundation for Food and Agriculture Research, and the U.K. Department for International Development under grant number OPP1172157. The authors wish to thank George Goodwin (Elsoms Seeds Ltd.) and Graham Teakle (Warwick Crop Centre) for providing seeds; Dr. Shaun Nielsen for discussions around R programming for model fitting; and two anonymous reviewers and Prof. A.P.M. Weber for constructive feedback that improved the manuscript.

Data availability statement

Data for leaf biochemistry, steady state responses to PPFD and CO₂, induction responses and dynamic A/c_i responses, are available at <https://doi.org/10.17635/lancaster/researchdata/378>

Conflict of interest

The authors declare that they have no conflict of interest

References

- Acevedo-Siaca L.G., Coe R., Wang Y., Kromdijk J., Quick W.P. & Long S.P. (2020) Variation in photosynthetic induction between rice accessions and its potential for improving productivity. *New Phytologist* <https://doi.org/10.1111/nph.16454>.
- Bradford M.M. (1976) A rapid and sensitive method for the quantitation of microgram quantities of protein utilizing the principle of protein-dye binding. *Analytical Biochemistry* **72**, 248–254.
- Burgess A.J., Retkute R., Preston S.P., Jensen O.E., Pound M.P., Pridmore T.P., & Murchie E.H. (2016) The 4-dimensional plant: Effects of wind-induced canopy movement on light fluctuations and photosynthesis. *Frontiers in Plant Science*, **7**, 1–12.
- von Caemmerer S. & Farquhar G.D. (1981) Some relationships between the biochemistry of photosynthesis and the gas exchange of leaves. *Planta* **153**, 376–387.
- von Caemmerer S. & Edmondson D. (1986). Relationship between steady-state gas exchange, *in vivo* Ribulose Bisphosphate Carboxylase activity and some carbon reduction cycle intermediates in *Raphanus sativus*. *Australian Journal of Plant Physiology*, **13**, 669–688.
- Carmo-Silva A.E. & Salvucci M.E. (2013) The regulatory properties of Rubisco Activase differ among species and affect photosynthetic induction during light transitions. *Plant Physiology* **161**, 1645–1655.
- Carmo-Silva E., Andralojc P.J., Scales J.C., Driever S.M., Mead A., Lawson T., ... Parry M.A.J. (2017) Phenotyping of field-grown wheat in the UK highlights contribution of light response of photosynthesis and flag leaf longevity to grain yield. *Journal of Experimental Botany* **68**, 3473–3486.

- Chazdon R.L. & Pearcy R.W. (1986) Photosynthetic responses to light variation in rainforest species I. Induction under constant and fluctuating light conditions. *Oecologia* **69**, 524–531.
- Cowan I.R. (1982) Regulation of water use in relation to carbon gain in higher plants. In *Encyclopedia of Plant Physiology New Series Volume 12 B*. (eds O.L. Lange, P.S. Nobel, C.B. Osmond & H. Ziegler), pp. 589–614. Springer Verlag, Berlin, Heidelberg, New York.
- Cowan I.R. & Farquhar G.D. (1977) Stomatal function in relation to leaf metabolism and environment. In *Symposia of the Society for Experimental Biology*. pp. 471–505.
- Deans R.M., Farquhar G.D. & Busch F.A. (2019a) Estimating stomatal and biochemical limitations during photosynthetic induction. *Plant, Cell & Environment*, **42**, 3227–3240.
- Deans R.M., Brodribb T.J., Busch F.A. & Farquhar G.D. (2019b) Plant water-use strategy mediates stomatal effects on the light induction of photosynthesis. *New Phytologist* **222**, 382–395.
- Farquhar G.D., von Caemmerer S. & Berry J.A. (1980) A Biochemical Model of Photosynthetic CO₂ Assimilation in Leaves of C₃ Species. *Planta* **149**, 78–90.
- Farquhar G.D. & Sharkey T.D. (1982) Stomatal Conductance and Photosynthesis. *Annual Review of Plant Physiology* **33**, 317–345.
- Fowler D., Coyle M., Skiba U., Sutton M.A., Cape J.N, Reis S., ... Voss M. (2013) The global nitrogen cycle in the twenty-first century. *Philosophical Transactions of the Royal Society B* **368**, 20130164.
- Glowacka K., Kromdijk J., Kucera K., Xie J., Cavanagh A.P., Leonelli L., ... Long S.P. (2018) Photosystem II Subunit S overexpression increases the efficiency of water use in a field-grown crop. *Nature Communications* **9**, article number 868.

- Gu L., Pallardy S.G., Tu K., Law B.E. & Wullschleger S.D. (2010) Reliable estimation of biochemical parameters from C_3 leaf photosynthesis-intercellular carbon dioxide response curves. *Plant, Cell and Environment* **33**, 1852–1874.
- Haddeland I., Heinke J., Biemans H., Eisner S., Florke M., Hanasaki N., ... Wissler D. (2014) Global water resources affected by human interventions and climate change. *Proceedings of the National Academy of Sciences of the United States of America* **111**, 3251-3256.
- Hammond E.T., John Andrews T., Mott K.A. & Woodrow I.E. (1998) Regulation of Rubisco activation in antisense plants of tobacco containing reduced levels of Rubisco activase. *Plant Journal* **14**, 101–110.
- Hanson D.T., Stutz S.S. & Boyer J.S. (2016). Why small fluxes matter: The case and approaches for improving measurements of photosynthesis and (photo)respiration. *Journal of Experimental Botany*, **67**, 3027–3039.
- Hermida-Carrera, C., Kapralov, M. V, & Galmés, J. (2016). Rubisco catalytic properties and temperature response in crops. *Plant Physiology*, *171*(August), pp.01846.2016
- Hikosaka K. & Terashima I. (1995) A model of the acclimation of photosynthesis in the leaves of C_3 plants to sun and shade with respect to nitrogen use. *Plant, Cell & Environment* **18**, 605–618.
- Inaba R. & Nishio T. (2002) Phylogenetic analysis of Brassiceae based on the nucleotide sequences of the S-locus related gene, SLR1. *Theoretical and Applied Genetics* **105**, 1159–1165.
- Indermühle A., Stocker T.F., Joos F., Fischer H., Smith H.J., Wahlen M., ... Stauffer B. (1999) Holocene carbon-cycle dynamics based on CO_2 trapped in ice at Taylor Dome, Antarctica. *Nature* **398**, 121–126.

- Kaiser E., Morales A., Harbinson J., Kromdijk J., Heuvelink E. & Marcelis L.F.M. (2015) Dynamic photosynthesis in different environmental conditions. *Journal of Experimental Botany* **66**, 2415–2426.
- Kaiser E., Morales A., Harbinson J., Heuvelink E., Prinzenberg A.E. & Marcelis L.F.M. (2016) Metabolic and diffusional limitations of photosynthesis in fluctuating irradiance in *Arabidopsis thaliana*. *Scientific Reports* **6**, 31252.
- Kaiser E., Kromdijk J., Harbinson J., Heuvelink E. & Marcelis L.F.M. (2017) Photosynthetic induction and its diffusional, carboxylation and electron transport processes as affected by CO₂ partial pressure, temperature, air humidity and blue irradiance. *Annals of Botany* **119**, 191–205.
- Kirschbaum M.U.F. & Pearcy R.W. (1988) Gas exchange analysis of the relative importance of stomatal and biochemical factors in photosynthetic induction in *Alocasia macrorrhiza*. *Plant Physiology* **86**, 782–785.
- Kromdijk J, Glowacka K, Leonelli L, Gabilly ST, Iwai M, Niyogi KK, Long SP (2016) Improving photosynthesis and crop productivity by accelerating recovery from photoprotection. *Science* **354**, 857-861.
- Kromdijk J. & Long S.P. (2016) One crop breeding cycle from starvation ? How engineering crop photosynthesis for rising CO₂ and temperature could be one important route to alleviation. *Proceedings of the Royal Society B*, **283**, 20152578.
- Larson G., Piperno D.R., Allaby R.G., Purugganan M.D., Andersson L., Arroyo-Kalin M., ... Fuller D.Q. (2014) Current perspectives and the future of domestication studies. *Proceedings of the National Academy of Sciences of the United States of America* **111**, 6139–6146.
- Lawson T., & Vialet-Chabrand S. (2019). Speedy stomata, photosynthesis and plant water use efficiency. *New Phytologist*, **221**, 93–98.

- Liu S., Liu Y., Yang X., Tong C., Edwards D., Parkin I.A.P., ... Paterson A.H. (2014) The *Brassica oleracea* genome reveals the asymmetrical evolution of polyploid genomes. *Nature Communications* **5**, 3980.
- Long, S.P. & Hallgren, J.-E. (1993). Measurement of CO₂ assimilation by plants in the field and the laboratory. In *Photosynthesis and Production in a Changing Environment: a field and laboratory manual* (eds D.O. Hall, J.M.O. Scurlock, H.R. Bolhàr-Nordenkamp, R.C. Leegood & S.P. Long), pp. 62–94. Chapman & Hall, London, United Kingdom.
- Long S.P., Ainsworth E.A., Rogers A. & Ort D.R. (2004) Rising atmospheric carbon dioxide: plants face the future. *Annual Review of Plant Biology*, **55**, 591-628.
- McAusland L., Vialet-Chabrand S., Davey P., Baker N.R., Brendel O. & Lawson T. (2016) Effects of kinetics of light-induced stomatal responses on photosynthesis and water-use efficiency. *New Phytologist* **211**, 1209–1220.
- Morales A., Kaiser E., Yin X., Harbinson J., Molenaar J., Driever S.M. & Struik P.C. (2018) Dynamic modelling of limitations on improving leaf CO₂ assimilation under fluctuating irradiance. *Plant Cell and Environment* **41**, 589–604.
- Mott K.A. & Woodrow I.E. (2000) Modelling the role of Rubisco activase in limiting non-steady-state photosynthesis. *Journal of Experimental Botany* **51**, 399–406.
- Ort D.R., Merchant S.S., Alric J., Barkan A., Blankenship R.E., Bock R., ... Zhu X.G. (2015) Redesigning photosynthesis to sustainably meet global food and bioenergy demand. *Proceedings of the National Academy of Sciences* **112**, 8529–8536.
- Parkin I.A.P., Gulden S.M., Sharpe A.G., Lukens L., Trick M., Osborn T.C. & Lydiate, D.J. (2005). Segmental structure of the *Brassica napus* genome based on comparative analysis with *Arabidopsis thaliana*. *Genetics* **171**, 765–781.

- Pearcy R.W., Krall J.P. & Sassenrath-Cole G.F. (1996) Photosynthesis in fluctuating light environments. In *Photosynthesis and the Environment*. (ed N.R. Baker), pp. 321–346. Kluwer Academic Publishers, Netherlands.
- R Core Team (2018) R: A language and environment for statistical computing.
- Rakow G. (2004) Species Origin and Economic Importance of *Brassica*. In: Pua E.C., Douglas C.J. (eds) *Brassica. Biotechnology in Agriculture and Forestry* **54**, 3-12 Springer, Berlin, Heidelberg
- Rana D., Van Den Boogaart T., O'Neill C.M., Hynes L., Bent E., Macpherson L., ... Bancroft I. (2004) Conservation of the microstructure of genome segments in *Brassica napus* and its diploid relatives. *Plant Journal* **40**, 725–733.
- Raschke K. (1975) Stomatal action. *Annual Review of Plant Physiology* **26**, 309–340.
- Sage R.F. (1995) Was low atmospheric CO₂ during the pleistocene a limiting factor for the origin of agriculture. *Global Change Biology*, **1**, 93-106.
- Salesse-Smith C.E., Sharwood R.E., Busch F.A., Kromdijk J., Bardal V. & Stern D.B. (2018) Overexpression of Rubisco subunits with RAF1 increases Rubisco content in maize. *Nature Plants* **4**, 802-810.
- Salter W.T., Merchant A.M., Richards R.A., Trethowan R. & Buckley T.N. (2019) Rate of photosynthetic induction in fluctuating light varies widely among genotypes of wheat. *Journal of Experimental Botany* **70**, 2787–2796.
- Sassenrath-Cole G.F. & Pearcy R.W. (1992) The role of ribulose-1,5-bisphosphate regeneration in the induction requirement of photosynthetic CO₂ exchange under transient light conditions. *Plant Physiology* **99**, 227–234.
- Sharwood R.E., Sonawane B.V., Ghannoum O. & Whitney S.M. (2016) Improved analysis of C₄ and C₃ photosynthesis via refined *in vitro* assays of their carbon fixation biochemistry. *Journal of Experimental Botany* **67**, 3137–3148.

- Sharkey T.D., Bernacchi C.J., Farquhar G.D. & Singsaas E.L. (2007) Fitting photosynthetic carbon dioxide response curves for C₃ leaves. *Plant, Cell and Environment* **30**, 1035-1040.
- Soleh M.A., Tanaka Y., Kim S.Y., Huber S.C., Sakoda K. & Shiraiwa T. (2017) Identification of large variation in the photosynthetic induction response among 37 soybean [*Glycine max* (L.) Merr.] genotypes that is not correlated with steady-state photosynthetic capacity. *Photosynthesis Research* **131**, 305–315.
- Soleh M.A., Tanaka Y., Nomoto Y., Iwahashi Y., Nakashima K., Fukuda Y., ... Shiraiwa T. (2016) Factors underlying genotypic differences in the induction of photosynthesis in soybean [*Glycine max* (L.) Merr.]. *Plant, Cell & Environment* **39**, 685–693.
- De Souza A.P., Wang Y., Orr D.J., Carmo-Silva E. & Long S.P. (2020) Photosynthesis across African cassava germplasm is limited by Rubisco and mesophyll conductance at steady state, but by stomatal conductance in fluctuating light. *New Phytologist* **225**, 2498-2512.
- Stephenson P., Baker D., Girin T., Perez A., Amoah S., King G.J. & Østergaard L. (2010) A rich TILLING resource for studying gene function in *Brassica rapa*. *BMC Plant Biology* **10**, 1–10.
- Tanaka Y., Adachi S. & Yamori W. (2019) Natural genetic variation of the photosynthetic induction response to fluctuating light environment. *Current Opinion in Plant Biology* **49**, 52–59.
- Taylor S.H. & Long S.P. (2017) Slow induction of photosynthesis on shade-sun transitions in wheat may cost at least 21% of productivity. *Philosophical Transactions of the Royal Society B: Biological Sciences* **372**, 20160543.

- Terashima I., Fujita T., Inoue T., Chow W.S. & Oguchi R. (2009) Green light drives leaf photosynthesis more efficiently than red light in strong white light: revisiting the enigmatic question of why leaves are green. *Plant & Cell Physiology* **50**, 684–697.
- Tilman D., Balzer C., Hill J. & Befort B.L. (2011) Global food demand and the sustainable intensification of agriculture. *Proceedings of the National Academy of Sciences of the United States of America* **108**, 20260–20264.
- Townsend A.J., Retkute R., Chinnathambi K., Randall J.W.P., Foulkes J., Carmo-Silva E. & Murchie E.H. (2018) Suboptimal acclimation of photosynthesis to light in wheat Canopies. *Plant Physiology* **176**, 1233–1246.
- Wang Y., Burgess S.J., de Becker E., & Long S.P. (2020). Photosynthesis in the fleeting shadows: An overlooked opportunity for increasing crop productivity? *The Plant Journal* **101**, 874–884.
- Wintermans J.F.G.M. & De Mots A. (1965) Spectrophotometric characteristics of chlorophylls a and b and their phenophytins in ethanol. *Biochimica et Biophysica Acta (BBA) - Biophysics including Photosynthesis* **109**, 448–453
- Woodrow I.E., Kelly M. & Mott K.A. (1996) Limitation of the rate of ribulosebisphosphate carboxylase activation by carbamylation and ribulosebisphosphate carboxylase activase activity: development and tests of a mechanistic model. *Australian Journal of Plant Physiology* **23**, 141-149.
- Woodrow I.E. & Mott K.A. (1989) Rate limitation of non-steady-state photosynthesis by ribulose-1,5-bisphosphate carboxylase in spinach. *Australian Journal of Plant Physiology* **16**, 487–500.

- Yamori W., Masumoto C., Fukayama H. & Makino A. (2012) Rubisco activase is a key regulator of non-steady-state photosynthesis at any leaf temperature and, to a lesser extent, of steady-state photosynthesis at high temperature. *The Plant Journal* **71**, 871–880.
- Yoon D.-K., Ishiyama K., Suganami M., Tazoe Y., Watanabe M., Imaruoka S., ... Makino A. (2020). Transgenic rice overproducing Rubisco exhibits increased yields with improved nitrogen-use efficiency in an experimental paddy field. *Nature Food*, **1**, 134–139.
- Zhu X.G., Ort D.R., Whitmarsh J. & Long S.P. (2004) The slow reversibility of photosystem II thermal energy dissipation on transfer from high to low light may cause large losses in carbon gain by crop canopies: A theoretical analysis. *Journal of Experimental Botany* **55**, 1167–1175.
- Zhu X.G., Long S.P. & Ort D.R. (2010) Improving photosynthetic efficiency for greater yield. *Annual Review of Plant Biology* **61**, 235–61.
- Zuur A.F., Ieno E.N., Walker N.J., Saveliev A.A. & G M Smith (2009) *Mixed Effects Models and Extensions in Ecology with R*. (eds M. Gail, K. Krickeberg, J.M. Samet, A. Tsiatis & W Wong), Springer, New York.

Table 1 Rubisco amount, specific and total activity for three *Brassica* (mean \pm SEM, N = 5).

Species	Rubisco total activity ($\mu\text{mol m}^{-2} \text{s}^{-1}$)	Rubisco amount (g m^{-2})	Rubisco specific activity ($\mu\text{mol g}^{-1} \text{s}^{-1}$)	Total soluble protein (g m^{-2})	Chlorophylls a and b (g m^{-2})	Chlorophyll a:b
<i>B. oleracea</i>	38 \pm 4.0	1.61 \pm 0.322	25.5 \pm 2.37	3.88 \pm 0.218 ^a	0.500 \pm 0.025 ^a	2.14 \pm 0.051 ^a
<i>B. napus</i>	46 \pm 3.6	1.79 \pm 0.147	26.1 \pm 0.86	4.83 \pm 0.266 ^b	0.428 \pm 0.025 ^a	2.28 \pm 0.02 ^{ab}
<i>B. rapa</i>	48 \pm 4.9	1.87 \pm 0.23	25.7 \pm 0.62	3.77 \pm 0.185 ^a	0.290 \pm 0.014 ^b	2.42 \pm 0.049 ^b

Different superscripts indicate significant differences at $P < 0.05$ using Tukey's HSD.

Table 2 Steady-state values for leaf net CO_2 assimilation (A), stomatal conductance to H_2O (g_{sw}), intrinsic water use efficiency ($i\text{WUE} = A/g_{\text{sw}}$), intercellular $[\text{CO}_2]$ (c_i), c_i for the limitation-state transition from $V_{\text{c,max}}$ to J ($c_{i,\text{trans}}$), and stomatal limitation (L_S) of three *Brassica*, at: PPFD, 1500 $\mu\text{mol m}^{-2} \text{s}^{-1}$; leaf temperature, 25 $^\circ\text{C}$; and leaf-air vapour pressure deficit, 1.2 kPa, and $\text{CO}_2 \sim 400 \mu\text{mol mol}^{-1}$ (mean \pm SEM, N = 4).

Species	A ($\mu\text{mol m}^{-2} \text{s}^{-1}$)	g_{sw} ($\text{mol m}^{-2} \text{s}^{-1}$)	c_i (Pa)	$c_{i,\text{trans}}$ (Pa)	L_S (%)
<i>B. oleracea</i>	32.5 \pm 0.69 ^a	0.46 \pm 0.055 ^a	26.5 \pm 0.95	35.1 \pm 1.55 ^a	21.9 \pm 2.24 ^a
<i>B. napus</i>	36.6 \pm 1.67 ^{ab}	0.63 \pm 0.040 ^{ab}	28.3 \pm 0.40	31.6 \pm 2.07 ^{ab}	14.5 \pm 1.98 ^{ab}
<i>B. rapa</i>	37.7 \pm 0.44 ^b	0.75 \pm 0.071 ^b	29.3 \pm 1.04	28.8 \pm 0.7 ^b	12.8 \pm 2.21 ^b

Different superscripts indicate significant differences at $P < 0.05$ using Tukey's HSD.

Table 3 Statistical summary of photosynthetic induction characteristics in three *Brassica*.Mean \pm SEM (N = 3, *B. oleracea*; N = 4, *B. napus* & *B. rapa*).

Species	<i>B. oleracea</i>	<i>B. napus</i>	<i>B. rapa</i>
Recovery in <i>A</i> at end of fast phase: two minutes after shade (R_{fast} , %)	64 \pm 4.9	72 \pm 4.8	72 \pm 3.2
Recovery in <i>A</i> , at c_i minimum ($R_{c_i,min}$, %)	77 \pm 5.0	81 \pm 3.7	84 \pm 3.5
Slow phase recovery ($R_{c_i,min} - R_{fast}$, %)	12.6 \pm 0.77	10 \pm 2.41	11.8 \pm 1.81
Time to c_i minimum* ($t_{c_i,min}$, min)	5.2 \pm 0.59	4.1 \pm 0.34	4.6 \pm 0.34
Time to 90% recovery of <i>A</i> ($t_{A,90}$, min)	16.7 \pm 3.49 ^a	8.7 \pm 2.02 ^b	7.4 \pm 1.41 ^b
Duration of recovery associated with increasing c_i ($t_{A,90} - t_{c_i,min}$, min)	11.5 \pm 3.28 ^a	4.6 \pm 1.71 ^{ab}	2.75 \pm 2.2 ^b

Different superscripts indicate differences with $P < 0.1$ using Tukey's HSD.

Figure Captions

Fig. 1 Responses of photosynthesis to light, for three *Brassica* species: (a) *B. oleracea*; (b) *B. napus*; (c) *B. rapa*. Non-rectangular hyperbola parameters: effective quantum yield (ϕ), asymptotic gross CO₂ assimilation rate (A_{sat}), curvature (θ), and day respiration (R_d) are provided as mean \pm SEM (N=4) across models fit to independent replicates within each species. Lines represent combined parameter means, and two representative sets of data are shown.

Fig. 2 CO₂ response curves show that shifts in operating c_i , and the c_i at which the factor limiting net CO₂ assimilation rate transitions from $V_{c,\text{max}}$ to J , result in different biochemical limitations of steady state photosynthesis among three *Brassica* species: (a) *B. oleracea* (circles); (b) *B. napus* (diamonds); (c) *B. rapa* (triangles). Maximum net CO₂ assimilation rates attributable to carboxylation limited by Rubisco (A_C), electron transport (A_J), and triose phosphate utilisation (A_P); CO₂ compensation point (I); and c_i values marking transitions between biochemical limiting factors, are plotted relative to mean operating points (grey fill, SEM smaller than symbol size). Also shown, are mean \pm SEM (N=4) for maximum Rubisco limited carboxylation rate ($V_{c,\text{max}}$), electron transport rate (J), and triose phosphate utilisation (T_P). Shading distinguishes two example data sets per species. Models were fit to data for individual leaves before summarizing parameters.

Fig. 3 Induction of net CO₂ assimilation (A), stomatal conductance (g_{sw}), and intercellular CO₂ (c_i) for three *Brassica* species, responding to an abrupt shift in photosynthetic photon flux density (PPFD), to 1500 $\mu\text{mol m}^{-2} \text{s}^{-1}$ after 30 minutes at 150 $\mu\text{mol m}^{-2} \text{s}^{-1}$. Mean \pm SEM for (a) *B. oleracea* (N=3), (b) *B. napus* (N=4), (c) *B. rapa* (N=4). Dashed lines indicate steady state values obtained at 1500 $\mu\text{mol m}^{-2} \text{s}^{-1}$ PPFD prior to shade.

Fig. 4 Time dependence of $V_{c,max}$ (a-c) and $dV_{c,max}/dt$ (d) following induction for (a) *Brassica oleracea* (N = 4), (b) *B. napus* (N = 4), and (c) *B. rapa* (N = 3). Arrows indicate mean values for the time to recover 90% of A , measured in separate induction measurements at ambient $[CO_2]$ ($t_{A,90}$; Table 3).

Fig. 5 Post-shade response of transition c_i values ($c_{i,trans}$), at which biochemical limitation switches from maximum rate of carboxylation by Rubisco ($V_{c,max}$) to either rate of electron transport (A_C/A_J , open symbols) or triose phosphate limitation (A_C/A_P , closed symbols), and c_i measured during induction at ambient $[CO_2]$ (small grey symbols, see also Fig. 3). Where $c_i < c_{i,trans}$ supports $V_{c,max}$ limitation, and $c_i > c_{i,trans}$ limitation by factors other than $V_{c,max}$. (a) *Brassica oleracea* (N = 4), (b) *B. napus* (N = 4), and (c) *B. rapa* (N = 3). Steady-state $c_{i,trans}$ (dashed lines; Table 2), and time to recover 90% of A , measured in separate induction measurements at ambient $[CO_2]$ (arrows, $t_{A,90}$; Table 3), are shown for reference.

Fig. 1

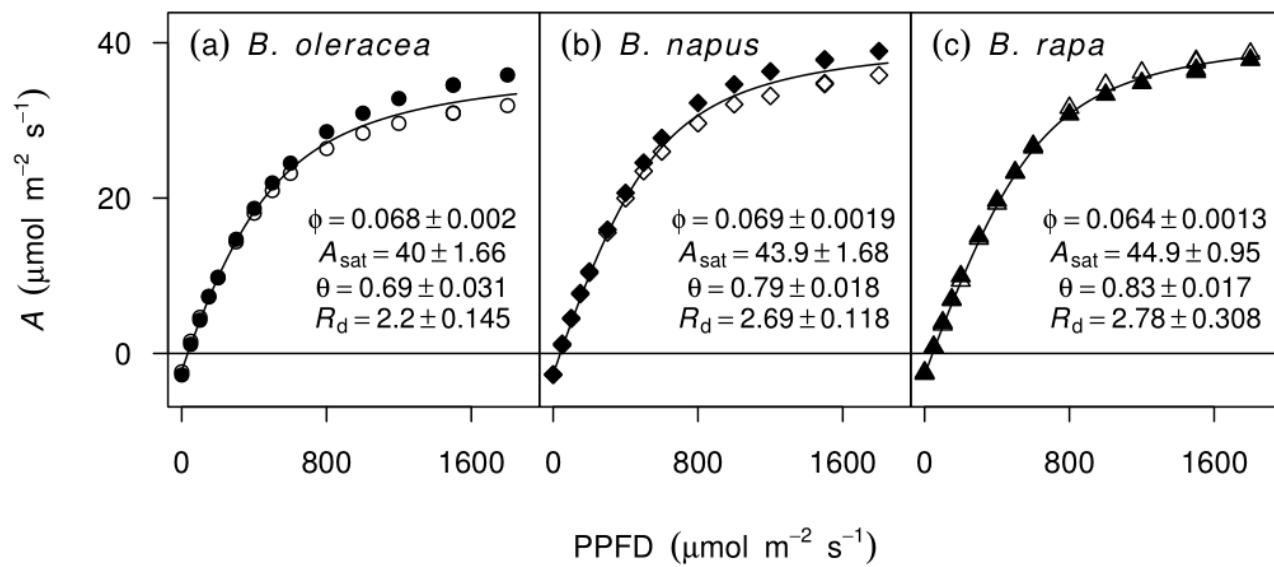


Fig. 2

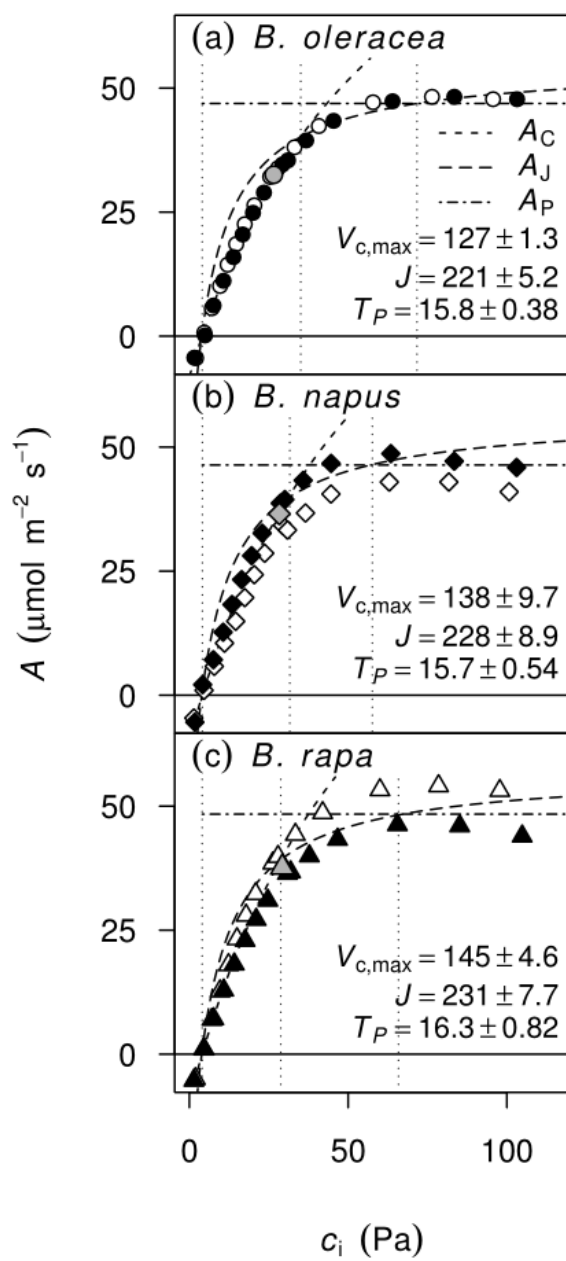


Fig. 3

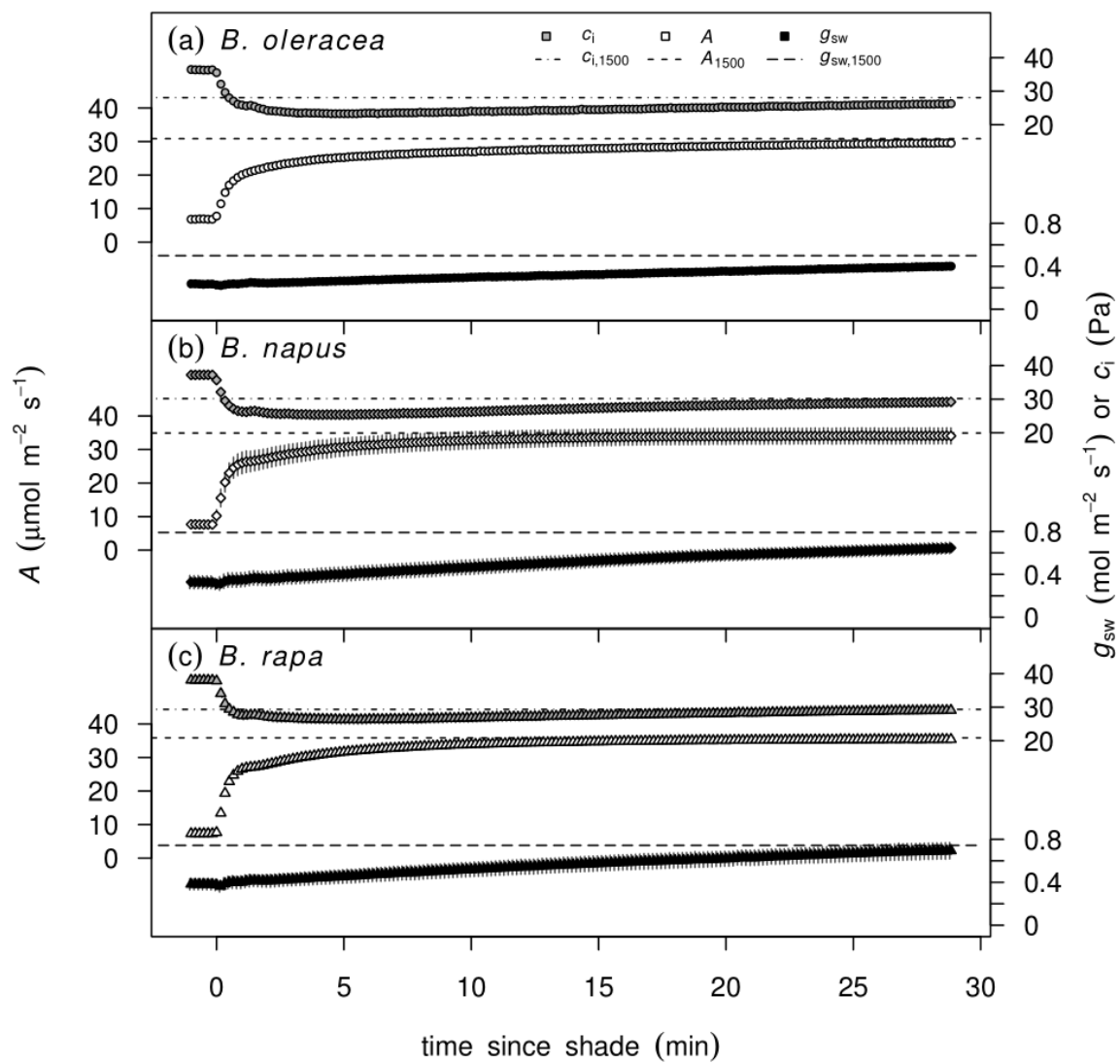


Fig. 4

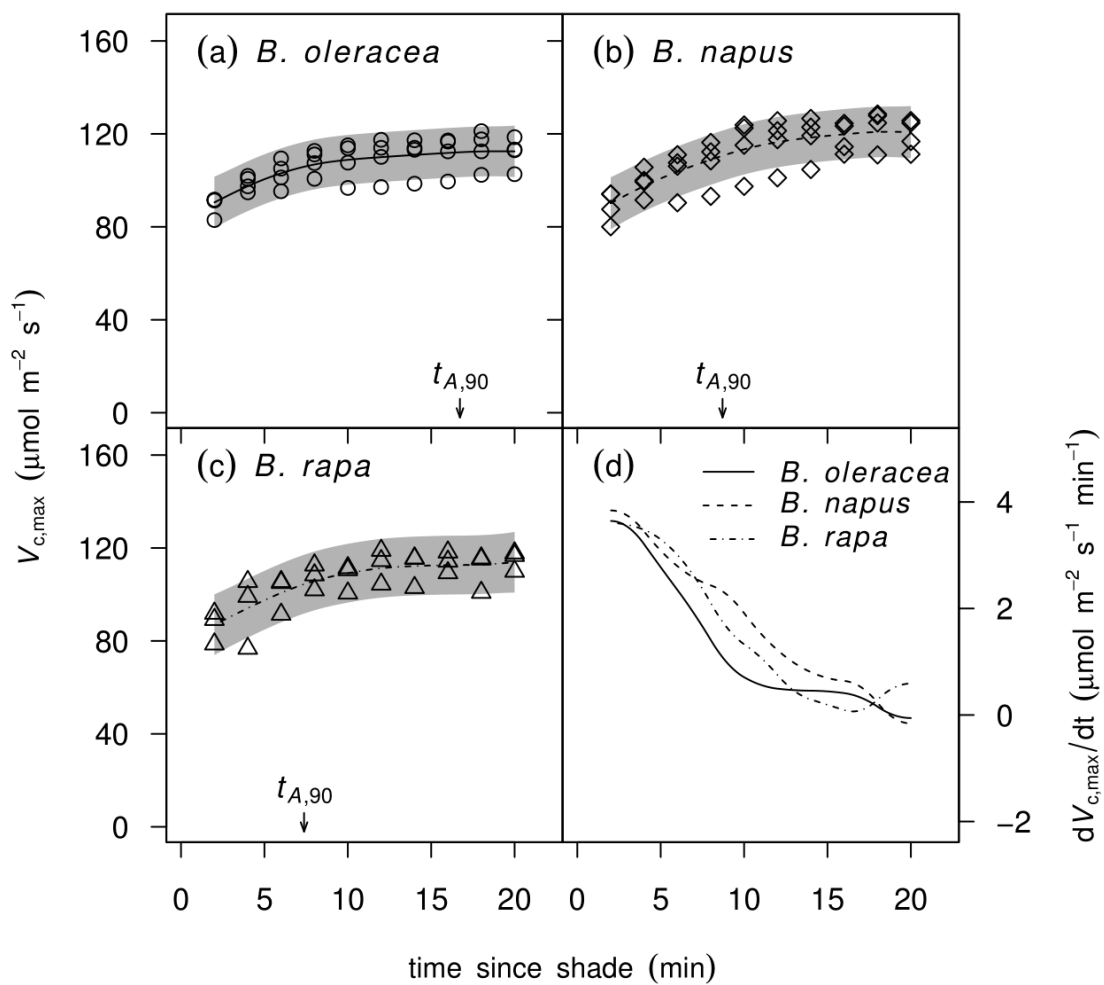


Fig. 5

